https://doi.org/10.1007/s41230-025-5009-x

Investigation on interfacial reaction and wettability between 4777DS1 superalloy and ceramic core

**Qiong-yuan Zhang[1, 3, 4], *Qiang Yang[2], A-tao Yang[1, 4], Ying-xin Wang[2], Jian He[1, 4], Yan Shang[2], Yu Fang[1, 4], and Qing-yan Xu[3]

1. State Key Laboratory of Clean and Efficient Turbomachinery Power Equipment, Deyang 618000, Sichuan, China

2. State Key Laboratory for Manufacturing System Engineering, School of Mechanical Engineering, Xi'an Jiaotong University, Xi'an 710049, China

3. School of Materials Sciences and Engineering, Tsinghua University, Beijing 100084, China

4. Dongfang Electric Corporation Dongfang Turbine Co., Ltd., Deyang 618000, Sichuan, China

Abstract: Low reactivity and appropriate wettability between molten superalloys and ceramic materials are crucial for the production of high-quality superalloy castings. The sessile-drop experiment was employed to systematically investigate the interfacial reaction and wettability between the 4777DS1 superalloy and SiO_2-based ceramic core at various temperatures (1,480 °C, 1,500 °C, 1,520 °C, and 1,550 °C). The wetting behavior and interfacial reaction products at different temperatures were analyzed by scanning electron microscopy (SEM), energy dispersive spectroscopy (EDS), and X-ray diffraction (XRD). The interfacial reaction process and products were discussed, and the thermodynamic behavior and interfacial reaction mechanisms were elucidated. The results demonstrate that the wetting behavior and interfacial reaction between the 4777DS1 alloy and the ceramic core are significantly influenced by temperature. The wettability angle exhibits a trend of initial decrease followed by an increase with rising temperature, reaching a maximum of 139° at 1,480 °C, indicating poorer wettability of the 4777DS1 superalloy with the ceramic core and better casting properties at this specific temperature. The most intense interfacial reaction occurs at 1,520 °C, resulting in the formation of the main interfacial reaction products such as Al_2O_3, SiO_2, and HfO_2. Additionally, some crystal-like products rich in Si and Hf distribute on the reaction layer.

Keywords: 4777DS1 superalloy; ceramic core; wettability; interfacial reaction

CLC numbers: TG146.1+5 **Document code:** A **Article ID:** 1672-6421(2026)02-205-10

1 Introduction

The improvement of thermal efficiency of modern industrial gas turbines (IGTs) mainly depends on the continuous increase of turbine inlet temperature. The thermal efficiency can be enhanced by 10% with a rise of 373 K of the turbine inlet temperature (TIT)[1]. The increase of TIT primarily relies on the improvement of blade cooling structures and blade grain structures[2-3]. However, the advancement of cooling technology has made the internal structure of hollow blades extremely complex, rendering traditional machining and electrochemical etching methods inadequate to meet manufacturing requirements[4-5]. The microstructure of superalloy blades has evolved from equiaxed grains to directionally columnar grains and now to single crystals, gradually eliminating grain boundaries between crystals, thereby enhancing the mechanical properties and service life of the blades[6-8]. Investment casting technology addresses the intricate challenges associated with the fabrication of complex air-cooling structures and facilitates the control of blade grain structures through the directional solidification process, thereby meeting the stringent manufacturing specifications required for high-performance turbine blades[9-10].

Ceramic core is a critical part in the process of manufacturing hollow turbine blade, as it ensures the formation of the cavity within the hollow turbine

*Qiang Yang

Male, born in 1987, Ph. D., Associate Researcher. His research interests mainly focus on additive manufacturing and preparation of single crystal turbine blades.

E-mail: qiangyang@xjtu.edu.cn

**Qiong-yuan Zhang

E-mail: zhangqiongyuan@dongfang.com

Received: 2025-01-14; Revised: 2025-02-23; Accepted: 2025-03-03

blade. It possesses superior comprehensive performance, including high temperature working capability, high dimensional stability, excellent thermal resistance, and excellent leachability[11-12]. Silicon-based ceramic core has been widely used in the investment casting of blade due to the advantages of low thermal expansion coefficient, good dimensional stability, and ease of removal[13]. However, in the actual production process of turbine blade, ceramic core needs to operate at high temperatures from 1, 500 °C to 1,600 °C for 1 to 2 h. During this period, the molten superalloy is in full contact with the ceramic core under high temperatures and high vacuum conditions, making the reactive elements in the superalloy susceptible to complex interfacial reactions with the oxides within the ceramic core[14-16]. These interfacial reactions can result in surface defects on the castings, including sand adhesions and porosities, which compromise the surface integrity of the castings and adversely affect their dimensional precision and suitability for further processing. Moreover, the formation of inclusions within the alloy can diminish the mechanical properties of the castings, significantly impacting the yield and quality of castings. With the development of superalloys, the content of refractory elements within these alloys is further increasing, leading to higher casting temperatures for fabrication of turbine blades by investment casting[17-18]. However, it is well known that higher temperatures enhance the rate of chemical reactions. Therefore, the higher casting temperatures will lead to more severe interfacial reactions between the molten superalloy and the ceramic core.

The interfacial reactions are closely related to wettability. It is crucial for the production of high-quality superalloy castings to have low reactivity and appropriate wettability between molten superalloys and ceramic materials, as reported by several studies[19-20]. Excessive wettability can lead to severe interfacial reactions due to the excessive contact between the molten superalloy and the ceramic core. Conversely, poor wetting leads to unqualified castings, which can result in casting defects such as gas porosity, inclusions, mold penetration, sweating, and the formation of oxide films[21-23]. Therefore, it is imperative to investigate the relationship between interfacial reactions and wettability to maintain the wettability between the superalloy melt and ceramic core material within an appropriate range.

In this study, the interfacial reaction and wettability between 4777DS1 superalloy and SiO_2-based ceramic core were systematically investigated. The wetting behavior and the interfacial reaction products at different temperatures were analyzed and studied in detail. Furthermore, the interfacial reaction process and reaction products were discussed. Meanwhile, the thermodynamic analysis and interfacial reaction mechanisms were clarified.

2 Materials and methods

2.1 Raw material

The 4777DS1 nickel-based superalloy was used as the raw material, and its chemical composition (wt.%) is shown in Table 1. The alloy was cut into 5 mm×5 mm×5 mm cubic samples by wire electrical discharge machining (WEDM), as shown in Fig. 1(a), then polished to remove traces of WEDM and ultrasonically cleaned in anhydrous ethanol to remove oil stains and oxides on the surface.

The ceramic substrate used for the experiments was the silica-based ceramic core manufactured by injection molding, which was comprised of 90wt.% SiO_2 and 10wt.% Al_2O_3. The ceramic core was sectioned into piece samples measuring 10 mm×10 mm×3 mm, as shown in Fig. 1(b). The XRD results of the surface of the ceramic core before the sessile-drop experiment are shown in Fig. 2. It can be seen from Fig. 2 that the initial phases of the ceramic core mainly consist of SiO_2, Al_2O_3, and a small amount of mullite ($3Al_2O_3{\cdot}2SiO_2$), which constitute the typical composition of silicon-based ceramic cores.

2.2 Sessile-drop experiment

The interfacial reaction and wettability experiments were carried out by using the sessile-drop method in a VIDF 15 vacuum directional solidification furnace (VIDF 15, Shenyang Vacuum Technology Institute Co., Ltd., China), as shown in Fig. 3(a). The ceramic substrate was positioned on the ceramic mold, with a layer of corundum sand interposed between them, to ensure a horizontal orientation. The 4774DS1 superalloy sample was then placed on the ceramic substrate. Subsequently, the furnace was evacuated to approximately 0.01 Pa, and then the temperature was increased at a rate of 20 °C·min^{-1} to reach target temperatures of 1,480 °C, 1,500 °C, 1,520 °C, and 1,550 °C to melt the alloy. Following a dwell time of 20 min, the alloy-ceramic couples were extracted from the furnace at a withdrawal rate of 7 mm·min^{-1} and subsequently cooled to room temperature. The alloy melt formed droplets approximately spherical in shape after directional solidification.

2.3 Characterization

After the sessile-drop experiment, the height (h) and the bottom diameter (d) of the alloy droplet were measured using a caliper, and the wettability angle of the molten alloy on the ceramic substrate was calculated using the geometric methods, as shown in Fig. 3(b).

When the droplet contacts the flat plate, assuming that the formed profile is an ellipse, an isosceles triangle ABC can be made based on the vertex A of the droplet observed from the

Table 1: Chemical composition of 4777DS1 nickel-based superalloy

Element	Cr	Co	Mo	W	Al	Ta	Ti	Hf	C	Ni
Weight percent (wt.%)	8.2	9.2	0.5	9.4	5.6	3.2	0.7	1.1	0.08	Bal.

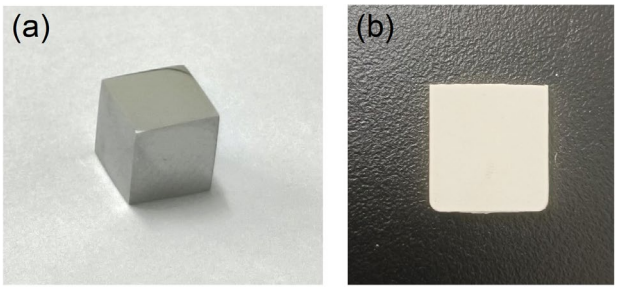

Fig. 1: Sessile-drop experiment samples: (a) 4777DS1 alloy; (b) ceramic core

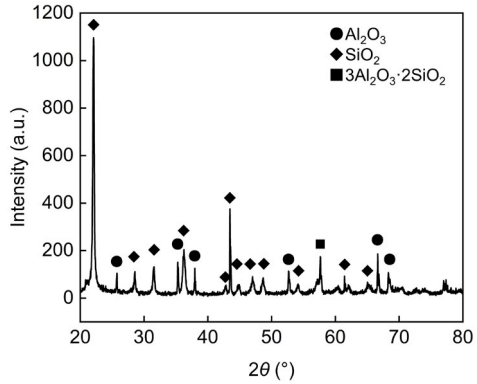

Fig. 2: Phase analysis of the surface of ceramic core before sessile-drop experiment

side, and the contact angle θ can be calculated using the h and d of the triangle[24]. In the triangle ADB, $\alpha+\beta=90°$, while $\theta=90°+(\beta-\alpha)$. Therefore, $\theta=\alpha+\beta+\beta-\alpha=2\beta$ can be obtained, then:

$$\tan\beta=2h/d \quad (1)$$

$$\theta=2\beta=2\arctan(2h/d) \quad (2)$$

The experiment was conducted by taking photos and then using Image Pro Plus to measure the β angle, and θ was calculated by using Eq. (2). To ensure the accuracy of the experimental results and reduce the impact of the non-perfect spherical shape on the measurement of the wettability angle, the wettability angle for each sample was measured and calculated three times (with an error range of ±2°), and the average of the three results was taken as the final wettability angle.

The analysis samples of interfacial reaction were extracted at room temperature. The microstructures of the alloy drop and the ceramic substrate were investigated by using a scanning electron microscope (SEM, Zeiss Sigma300, Carl Zeiss AG, Oberkochen, Germany) equipped with an energy dispersive spectroscope (EDS). The surface composition analysis of the alloy drops and the ceramic core samples was conducted by using the EDS. The X-ray diffraction (XRD, D8 Advance, Bruker AXS GmbH, Karlsruhe, Germany) was used to detect

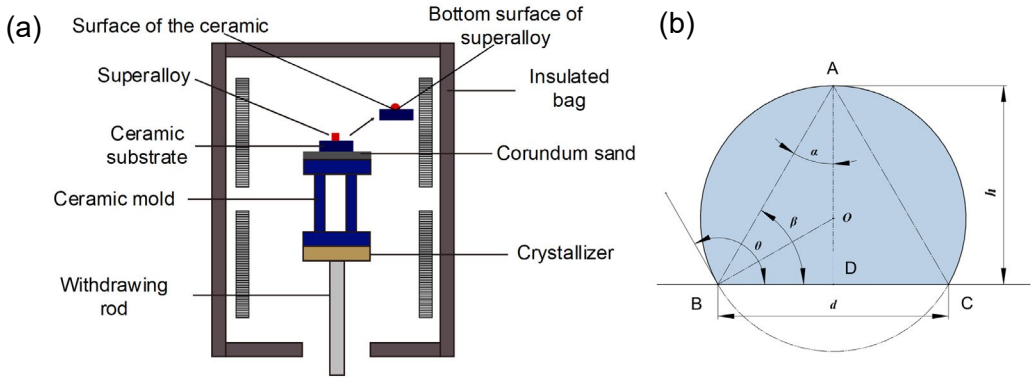

Fig. 3: Schematic diagram of the sessile-drop experiment (a) and measurement method for alloy-ceramic wetting angles (b)

and analyze the phase constitution of the alloy, ceramic materials, and the interface between the superalloy and the ceramic.

3 Results and discussion

3.1 Wetting behavior

Figure 4 shows the changes in the wetting angle of the 4777DS1 superalloy on the ceramic substrate across various temperatures. It can be observed that as the temperature varies among 1,480 °C, 1,500 °C, 1,520 °C, and 1,550 °C, the wetting angle undergoes obvious changes, with respect values of 139°, 129.5°, 125.4°, and 132.1°. The results indicate that as the temperature increases, the wetting angle gradually decreases with the temperature rising from 1,480 °C to 1,520 °C. However, when the temperature is further elevated to 1,550 °C, the wetting angle increases to 132.1°. At a temperature of 1,480 °C, the maximum wetting angle reaches 139° indicating that the wettability of the 4777DS1 superalloy on the ceramic core is relatively low. However, this specific temperature appears to favor better casting properties for the 4777DS1 superalloy.

3.2 Bottom surface morphology and phases analysis of 4777DS1 alloy drop

Figure 5 illustrates the microstructural morphology of the bottom surface of 4777DS1 alloy droplets following sessile-drop experiments conducted at various temperatures. At 1,480 °C, the interfacial reaction area on the bottom of the alloy droplet is significantly smaller, in which the area

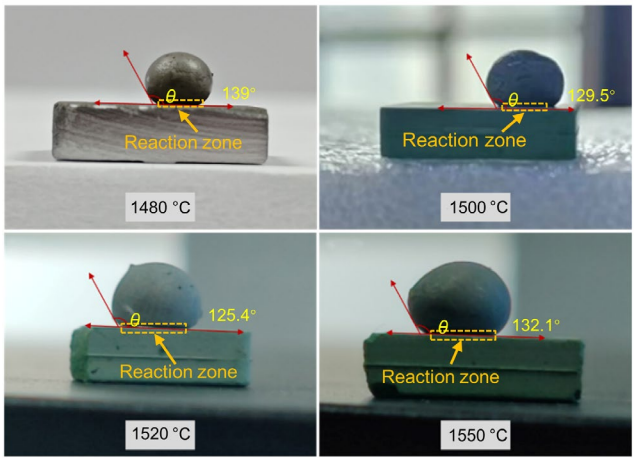

Fig. 4: Macro photographs of wettability angles between 4777DS1 alloy melt and ceramic core substrate at different temperatures

is relatively smooth and no obvious sand sticking observed, compared to the areas observed at other temperatures. The bottom of the alloy droplet is coated with a minimal amount of reaction products. However, the bottoms of the alloy drops obtained at 1,500 °C, 1,520 °C, and 1,550 °C are extensively coated with reaction products, even local peeling of reaction layer is observed. This observation preliminarily suggests that the alloy droplets have undergone different extents of interfacial reactions with the SiO_2-based ceramic core.

To precisely characterize the composition of the reaction products, XRD and EDS were employed to analyze the phases constituents and elemental compositions. Figure 6 shows the XRD phase analysis results of the interfacial reaction on the bottom surface of 4774DS1 alloy at different temperatures. As can be seen, the phases change with the variation of temperatures. At 1,480 °C, the phases of interfacial reaction are

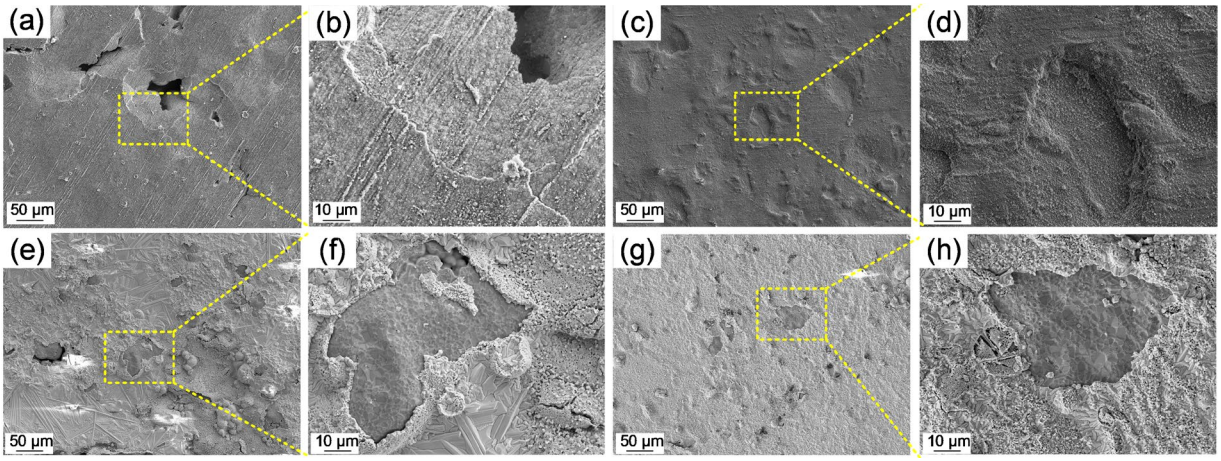

Fig. 5: Microscopic morphology of the bottom surface of 4777DS1 alloy drops after sessile-drop experiments: (a) and (b) 1,480 °C; (c) and (d) 1,500 °C; (e) and (f) 1,520 °C; (g) and (h) 1,550 °C

composed of SiO_2, Al_2O_3, which are the mainly components of the ceramic core. However, phases of interfacial reaction obtained in 1,500 °C, 1,520 °C, and 1,550 °C exhibite typical interface reaction products of HfO_2 on the bottom surface of 4774DS1 alloy drops, indicating that a relatively severe interface reaction occurred at these temperatures. The changes of phases correspond to the changes of microstructures observed in Fig. 5.

Figure 7 illustrates the microstructural morphology and the elemental distribution in the local region after the reaction between 4777DS1 alloy and ceramic core at 1,480 °C, 1,500 °C, 1,520 °C, and 1,550 °C. Figure 7(a) shows that at 1,480 °C, the bottom surface of the 4777DS1 alloy droplet consists of an interfacial reaction layer and an exposed alloy matrix. EDS analysis reveals that the reaction products are abundant in O and Al, with trace amounts of Si, Cr, and Ni, and relatively deficient in Hf. Combined with the XRD analysis results, it can be inferred that the primary substance adhering to the surface of the alloy is Al_2O_3, with minor amounts of SiO_2, and pores exist between the particles. In particular, the HfO_2 is barely detected. Figure 7(b) illustrates the microstructural morphology and the elemental distribution at 1,500 °C. Different from the reaction layer at 1,480 °C, the bottom surface of the alloy droplet consists of a dense interfacial reaction layer, without any exposed alloy matrix. The EDS analysis indicates that the reaction products are abundant in O, Al, and Hf, with trace amounts of Si, Cr, and Ni. Combined with the XRD analysis results, it can be inferred that the main substance adhered to the surface of the alloy is Al_2O_3 and HfO_2, with a little of SiO_2. The reaction layer is very dense, preventing other elements in the alloy from continuing to react with the ceramic core. Figure 7(c) illustrates the microstructural morphology and the elemental distribution in the local region after the reaction between 4777DS1 alloy and ceramic core at 1,520 °C. The bottom surface of the alloy drop consists of an interfacial reaction layer and a larger area of exposed alloy matrix. The EDS analysis indicates that the reaction products are abundant in O, Al, Si, and Hf, with trace amounts of Cr and Ni. Combined with the XRD analysis results, it can be inferred that the main substance adhered to the surface of the alloy drop is Al_2O_3, SiO_2, and HfO_2. Different from the reaction layer at 1,480 °C and 1,500 °C, there is a large area

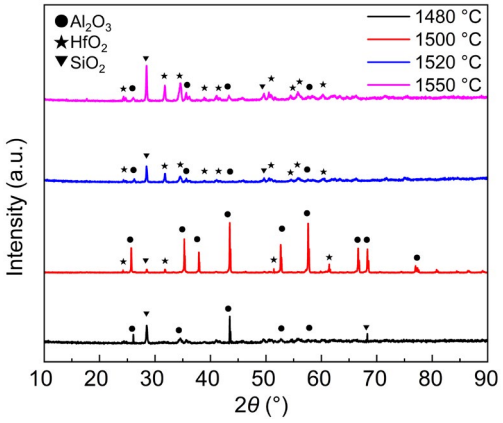

Fig. 6: Phase analysis of bottom surface of 4774DS1 alloy drops at different temperatures

of exposed alloy matrix, and the EDS result of this area shows rich in Ni and Cr elements, indicating that this is the exposed alloy matrix due to the local reaction layer peeled. In addition, some crystal-like products, indicated by arrows in Fig. 7(c), are rich in Si and Hf, and are distributed on the reaction layer, which may be inferred as $HfSiO_4$ formed by the reaction of SiO_2 and HfO_2 at a high temperature. Figure 7(d) illustrates the microstructural morphology and the elemental distribution in the local region after the reaction between 4777DS1 alloy and ceramic core at 1,550 °C. Similar to the reaction layer at 1,520 °C, the bottom surface of the alloy drop consists of an interfacial reaction layer and a larger area of exposed alloy matrix. The EDS analysis indicates that the reaction products are abundant in O, Al, Si, and Hf, with trace amounts of Cr and Ni. Combined with the XRD analysis results, it can be inferred

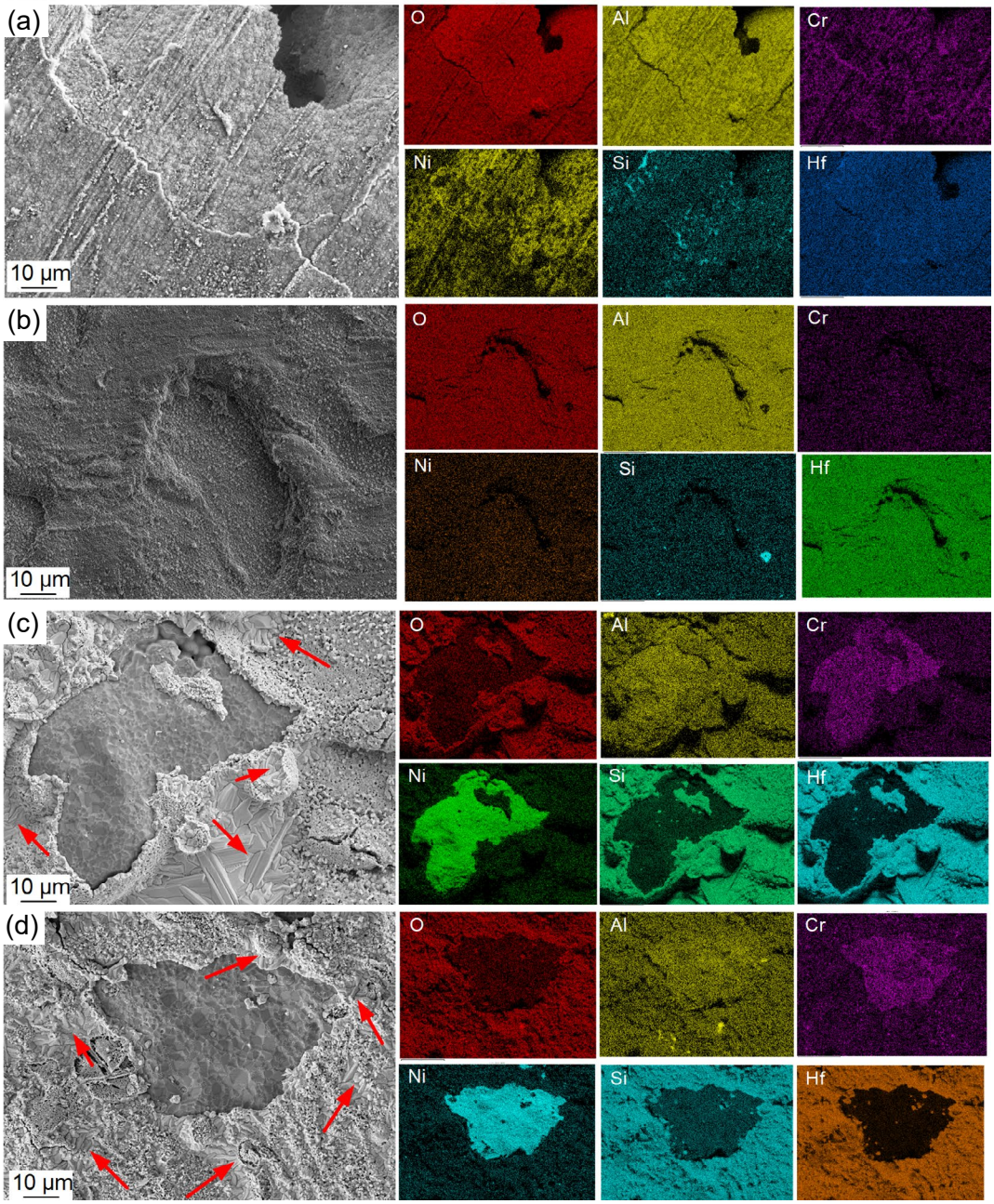

Fig. 7: Microstructure and element distribution of bottom surface of 4774DS1 alloy drops at different temperatures: (a) 1,480 °C; (b) 1,500 °C; (c) 1,520 °C; (d) 1,550 °C

that the main substance adhered to the surface of the alloy is Al_2O_3, SiO_2, and HfO_2, and the area rich in Ni and Cr elements is the exposed alloy matrix due to the local reaction layer peeled. The difference with that at 1,500 °C is that crystal-like products, indicated by arrows in Fig. 7(d), become smaller and more widely distributed in the reaction layer.

3.3 Surface morphology and phases analysis of silica-based ceramic core

Figure 8 depicts the microstructural morphology of the surface of the silica-based ceramic core following sessile-drop experiments conducted at various temperatures. As can be seen from Fig. 8, the surface of ceramic core obtained by sessile-drop experiments at different temperatures shows distinct sintered states along with areas where sand has adhered. It indicates that the ceramic core samples and the 4774DS1 superalloy drops exhibit varying degrees of interfacial reactivity. At 1,480 °C, the surface of ceramic core samples is very close to the initial surface of the core before sessile-drop experiment, displaying an initial state where Al_2O_3 particles are uniformly dispersed throughout the SiO_2 matrix, with the interfacial reaction products being rarely observed. However, the surface of the ceramic core samples obtained at 1,500 °C, 1,520 °C, and 1,550 °C exhibits characteristics indicative of re-sintering, with a microstructure that appears denser. Additionally, the surface is covered with some reaction products, even on the surface of the ceramic core obtained at 1,520 °C, a peeling reaction layer is detected.

Figure 9 shows the XRD phase analysis results of the surface of ceramic core at different temperatures. As can be seen from Fig. 9, the phases of interfacial reaction on the surface of ceramic core change with variational temperature. At 1,480 °C, the phase constitution of interfacial reaction is very similar to the initial phase of the core prior to sessile-drop experiment, primarily consisting of SiO_2, Al_2O_3, and a small amount of mullite ($3Al_2O_3{\cdot}2SiO_2$), indicating that no intense interface reaction occurrs at this temperature. However, the phases observed at interfacial reaction zone obtained at 1,500 °C, 1,520 °C, and 1,550 °C exhibit typical interface reaction products of HfO_2, indicating that a relatively severe interface reaction occurrs at these temperatures. The changes of phases correspond to the changes of microstructures observed in Fig. 8. The interfacial reaction is weak at 1,480 °C, however, the interfacial reactions are much more vigorous as the temperature increases to 1,500, 1,520, and 1,550 °C.

In order to elucidate the interfacial reaction products on the surface of the ceramic core, the microstructure morphologies and the element distribution in the local area of ceramic core samples after reacting with 4777DS1 alloy at different temperatures were detected using EDS, as shown in Fig. 10. Figure 10(a) illustrates that at 1,480 °C, the surface of ceramic core consists of an interfacial reaction layer and an exposed ceramic core matrix. The EDS analysis reveals that the reaction products are abundant in O, Si, and Al, while being relatively deficient in Cr, Ni, and Hf. Combined with the XRD analysis results, it can be inferred that the main interfacial reaction products on the surface of the ceramic core are SiO_2, Al_2O_3, and a small amount of mullite. The microstructure still retains the typical features of a ceramic core, with Al_2O_3 particles uniformly distributed throughout the SiO_2 matrix, which act as reinforcing phases. Pores are observed between the particles. Different from at 1,480 °C, the surface of the ceramic core is covered by a dense interfacial reaction layer at 1,500 °C, as shown in Fig. 10(b). The EDS analysis reveals that the reaction products remain rich in O, Si, and Al, with trace amounts of Hf, and relatively deficient of Cr and Ni. Combined with the XRD analysis results, it can be inferred that the main interfacial reaction products on the surface of the ceramic core are SiO_2, Al_2O_3, and HfO_2, along with a minor amount of mullite. When the temperature increases to 1,520 °C, the surface of the ceramic core consists of an interfacial reaction layer and a large spalled interfacial reaction product, as illstrated in Fig. 10(c). The reaction products are abundant in O, Si, Al, and Hf, with trace amounts of Cr and Ni. Especially, the spalled interfacial reaction products exhibit a significant enrichment of Hf elements. Based on the XRD analysis results, it can be inferred that the main interfacial reaction products on the surface of the ceramic core are SiO_2, Al_2O_3, HfO_2, and a minor amount of mullite, Cr_2O_3, and NiO,

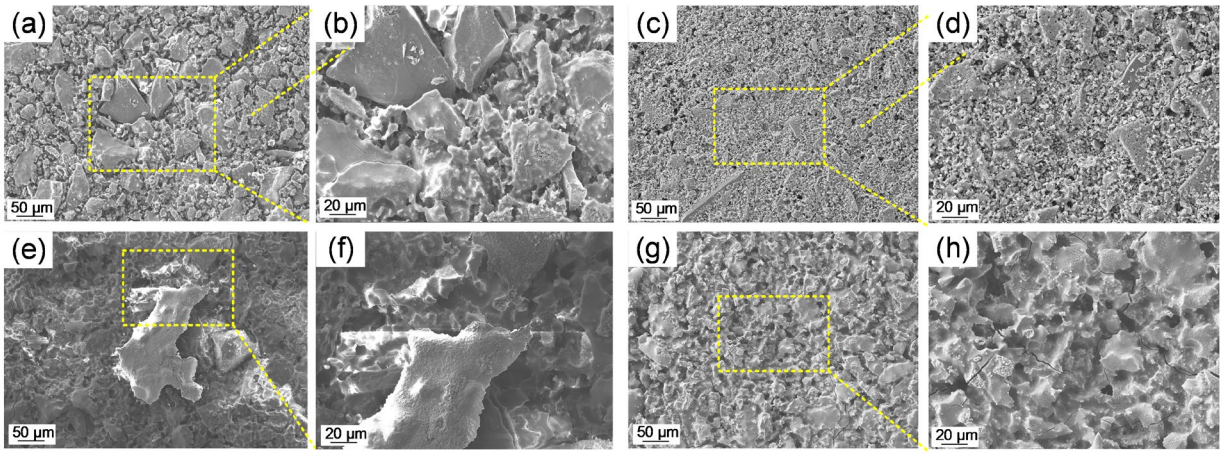

Fig. 8: Microscopic morphology of surface of ceramic core after sessile-drop experiments: (a) and (b) 1,480 °C; (c) and (d) 1,500 °C; (e) and (f) 1,520 °C; (g) and (h) 1,550 °C

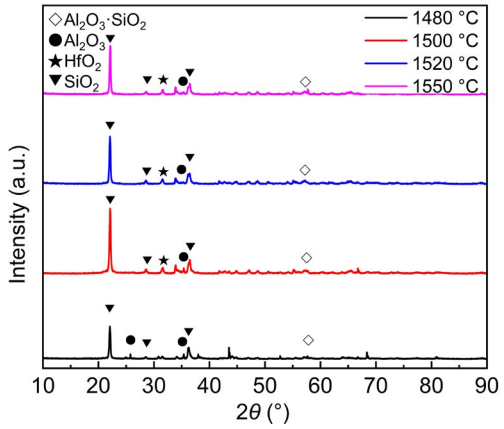

Fig. 9: Phase analysis of the surface of ceramic cores at different temperatures

which are not detected by XRD due to their low content. Different from the reaction layer at 1,480 °C and 1,500 °C, a large spalled interfacial reaction product is present at higher temperatures, and the elemental mapping by EDS in this area reveals a high concentration of Hf and O elements, indicating that the spalled material is HfO_2. This HfO_2 formation is a result of intense reaction between the 4777DS1 alloy and the ceramic core, leading to the peeling off of the reaction product from the alloy matrix. In addition, the microstructure of the ceramic core is denser than that of 1,480 °C and 1,500 °C, exhibiting a state of re-sintering. At 1,520 °C, as shown in Fig. 10(d), the microstructure of the ceramic core is denser than that at 1,480 °C, 1,500 °C, and 1,520 °C. The surface of the ceramic core is composed of an uniformly distributed interfacial reaction layer. The

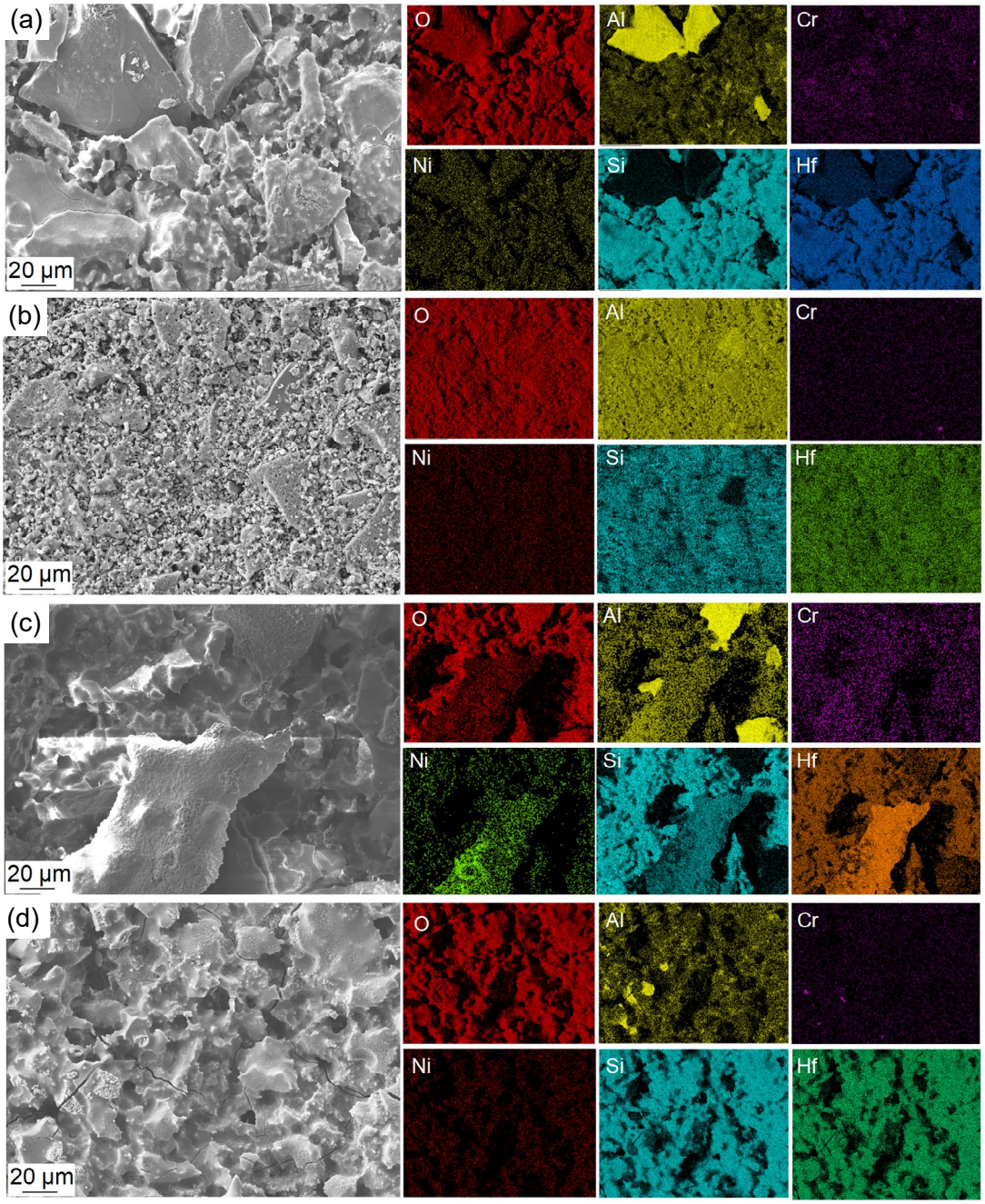

Fig. 10: Microstructure and element distribution of the surface of ceramic cores at different temperatures: (a) 1,480 °C; (b) 1,500 °C; (c) 1,520 °C; (d) 1,550 °C

reaction products are abundant in O, Al, Si, and Hf, but relatively deficient in Cr and Ni. Combined with the XRD analysis results, it can be inferred that the primary substances adhering to the surface of the ceramic core are SiO_2, Al_2O_3, and HfO_2. In contrast to the sample treated at 1,520 °C, Cr and Ni do not significantly participate in the interfacial reaction at this temperature. As a result, the reaction layer exhibits a more uniform distribution. This also indicates that at 1,550 °C, the reaction is less intense than that at 1,520 °C, which is consistent with the results of wettability.

3.4 Thermodynamic analysis and reaction mechanism of interfacial reactions

To further validate the accuracy of the analysis, the thermodynamic calculations of the interfacial reactions between the main elements of the 4777DS1 alloy and the SiO_2 and Al_2O_3 in the ceramic core were conducted. Gibbs free energy calculation is pivotal in material thermodynamic analysis[25]. Irrespective of the products formed from the interfacial reactions between the 4777DS1 alloy and the ceramic core, the thermodynamic condition of $\Delta G<0$ must be met as a prerequisite. A smaller value of ΔG indicates that the reaction is more likely to occur. The standard molar Gibbs free energy of formation, ΔG^{Θ}, can be calculated by combining Eqs. (3) and (4)[26]:

$$\Delta G^{\Theta}(T) = \Delta H^{\Theta}_{298} + \int_{298}^{T} \Delta C^{\Theta}_{p}\,\mathrm{d}T - T\Delta S^{\Theta}_{298} - T\int_{298}^{T} \frac{\Delta C^{\Theta}_{p}}{T}\mathrm{d}T \quad (3)$$

$$\Delta C^{\Theta}_{p} = a + bT + cT^{-2} \quad (4)$$

where, $\Delta G^{\Theta}(T)$ is the standard molar Gibbs free energy of formation at temperature T, ΔH^{Θ}_{298} is the standard molar enthalpy of formation, $\Delta C^{\Theta}_{p}(T)$ is the standard molar heat capacity at constant pressure difference between products and reactants, ΔS^{Θ}_{298} is the standard entropy change of the reaction. The a, b, and c are empirical constants[27]. The Gibbs free energy of reaction between the main elements of the 4777DS1 alloy and the SiO_2 and Al_2O_3 of the ceramic core at 1,000 °C to 1,600 °C were calculated and the results are shown in Fig. 11.

The results demonstrate that, within the temperature range of 1,000 °C to 1,100 °C, the propensity for interfacial reactions between the principal elements of the 4777DS1 alloy and the SiO_2 in the ceramic core is ordered from the greatest to least as follows: HfO_2>Al_2O_3>TiO_2>Ta_2O_5>Cr_2O_3>WO_3>CoO>NiO, however, within the temperature range of 1,100 °C to 1,600 °C, the propensity for interfacial reactions is ordered from the greatest to least as follows: HfO_2>TiO_2>Al_2O_3>Ta_2O_5>Cr_2O_3>WO_3>CoO>NiO. When considering the interfacial reactions between the principal elements of the 4777DS1 alloy and the Al_2O_3 in the ceramic core the propensity follows a similar trend, ranking from highest to lowest as follows: HfO_2>TiO_2>Ta_2O_5>Cr_2O_3>WO_3>CoO>NiO. Based on the thermodynamic calculations of Gibbs free energy, the propensity for interfacial reactions between the main elements of the 4777DS1 alloy and the ceramic core is found to be generally consistent with the products of the interfacial reactions previously discussed.

In reality, the interfacial reaction between the molten alloy and ceramic core is a complex process. It usually consists of four main steps[27]: (1) decomposition of active atoms from the superalloy material, as shown in Fig. 12(a); (2) dissolution or decomposition of active atoms from the ceramic core material, as shown in Fig. 12(b); (3) diffusion of active atoms from the alloy matrix and ceramic core to the alloy/ceramic interface, such as Hf element is actuated to the alloy/ceramic interface by temperature gradient[27], as shown in Fig. 12(c); (4) reaction products formation by substitution reaction at alloy/ceramic interface, as shown in Fig. 12(d).

4 Conclusions

This study mainly investigated the interfacial reaction and wettability between 4777DS1 superalloy and SiO_2-based ceramic core at different temperatures. The wetting behavior and the interfacial reaction products at different temperatures were analyzed and studied in detail. The following conclusions are drawn:

(1) The wetting behavior and the interfacial reaction between the 4777DS1 alloy and the ceramic core are significantly affected by temperatures. The wettability angle between the 4777DS1 alloy melt and the ceramic core shows a trend of

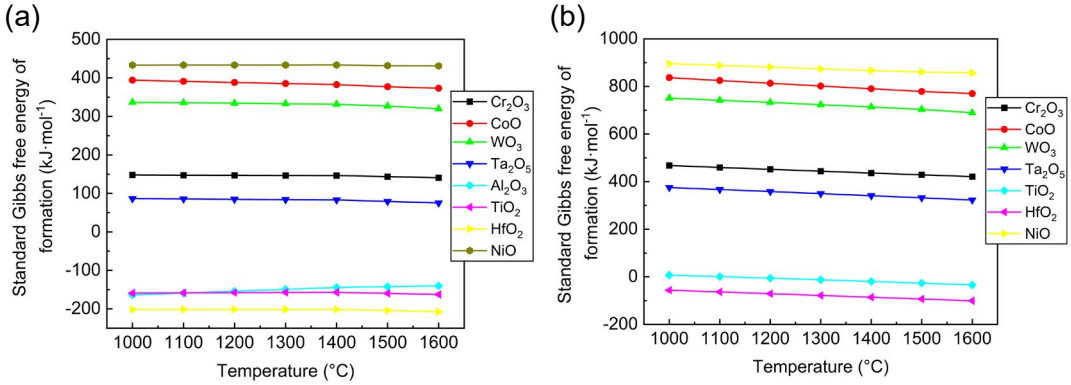

Fig. 11: Standard Gibbs free energy of possible reaction between main elements of 4777DS1 superalloy and ceramic core at temperatures ranging from 1,000 °C to 1,600 °C: (a) SiO_2; (b) Al_2O_3

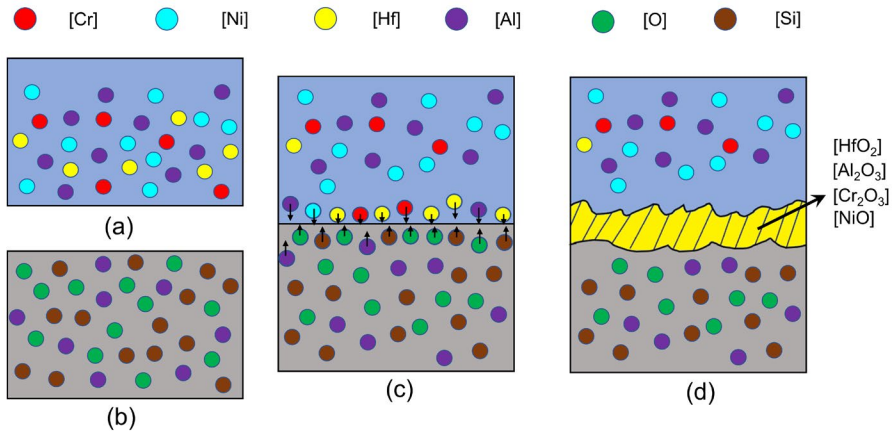

Fig. 12: Schematic illustration of interfacial reaction processes between 4777DS1 alloy and ceramic core: (a) atoms produced by dissolution of superalloy; (b) atoms produced by decomposition of ceramic core; (c) diffusion of active atoms from alloy matrix and ceramic core to alloy/ceramic interface; (d) reaction products formation by substitution reaction[27]

initially decreasing and then increasing as the temperature rises.

(2) The maximum wettability angle of 139º is obtained at a temperature of 1,480 °C, indicating that the 4777DS1 superalloy has relatively poorer wettability with the ceramic core. This suggests that the alloy has better casting properties at this temperature, as a higher wettability angle typically corresponds to less interaction and better flow characteristics during the casting process.

(3) The most intense interfacial reaction occurs at 1,520 °C, characterized by a minimum wettability angle of 125.4º. The main interfacial reaction products are Al_2O_3, SiO_2, and HfO_2. Additionally, some crystal-like products, which are rich in Si and Hf, distribute on the reaction layer.

Acknowledgments

This work was supported by the fund of State Key Laboratory of Clean and Efficient Turbomachinery Power Equipment (No. DEC8300CG202210353EE280297), the China Postdoctoral Science Foundation (No. 2021M692555), the Shaanxi Province Qinchuangyuan 'Scientists+Engineers' Team Building Project (No. 2023KXJ-266), and the Fundamental Research Funds for the Central Universities (No. xzy012023145).

Conflict of interest

The authors declare that they have no known competing financial interests or personal relationships that could have appeared to influence the work reported in this paper.

References

[1] Reed R C. The superalloys: Fundamentals and applications. London: Cambridge University Press, 2006.

[2] Wang H Z, Long H B, Sun M, et al. Effect of directional solidification methods on solid solution window in Ni-based single-crystal superalloy. Journal of Materials Research and Technology, 2023, 24: 8307–8319.

[3] Shang Z, Wei X P, Song D Z, et al. Microstructure and mechanical properties of a new nickel-based single crystal superalloy. Journal of Materials Research and Technology, 2020, 9(5): 11641–11649.

[4] Zhang G H, Zhu R, Xie G N, et al. Optimization of cooling structures in gas turbines: A review. Chinese Journal of Aeronautics, 2022, 35(6): 18–46.

[5] Xu L, Sun Z N, Ruan Q C, et al. Development trend of cooling technology for turbine blades at super-high temperature of above 2000 K. Energies, 2023, 16(2): 668.

[6] Zhang C J, Zhou Y L, Shi C X, et al. Study on the dendritic growth and grain boundary formation in the suddenly expanded cross-section of single crystal superalloy during directional solidification process. Journal of Manufacturing Processes, 2024, 127: 764–778.

[7] Chen Y, Yao Z H, Wang J J, et al. Microstructural evolution and diffusion mechanism of MCrAlY coated nickel-based superalloy turbine blades after serviced for 47000 h. Surface and Coatings Technology, 2024, 493: 131288.

[8] Wang F, Liu Y, Yang Q, et al. Microscale stray grains formation in single-crystal turbine blades of Ni-based superalloys. Journal of Materials Science and Technology, 2024, 191: 134–145.

[9] Ma D X, Wang F, Wu Q, et al. Innovations in casting techniques for single crystal turbine blades of superalloys. Superalloys, 2016: 237–246.

[10] Pattnaik S, Karunakar D B, Jha P K. Developments in investment casting process: A review. Journal of Materials Processing Technology, 2012, 212(11): 2332–2348.

[11] Chauhan A S, Anirudh B, Satyanarayana A, et al. FEA optimization of injection parameters in ceramic core development for investment casting of a gas turbine blade. Materials Today: Proceedings, 2020, 26: 2190–2199.

[12] Yang Q, Wang F, Li D C. Effect of chopped ZrO_2 fiber content on the microstructure and properties of CaO-based integral ceramic mold. Materials, 2020, 13(23): 5398.

[13] Wang X G, Zhou Y L, Zhou L, et al. Microstructure and properties evolution of silicon-based ceramic cores fabricated by 3D printing with stair-step effect control. Journal of the European Ceramic Society, 2021, 41(8): 4650–4657.

[14] Zheng L, Xiao C B, Zhang G Q, et al. Investigation of interfacial reaction between high Cr content cast nickel-based superalloy K4648 and ceramic cores. Journal of Aeronautical Materials, 2012, 32(3): 10–22.

[15] Zhao J Q, Li Y, Tan Y, et al. Effects of surface-active elements on wettability and interfacial reaction between DD5 superalloy and Al_2O_3-based ceramic shell. Results in Surfaces and Interfaces, 2024, 17: 100325.
[16] Xuan W D, Du L F, Song G, et al. Some new observations on interface reaction between nickel-based single crystal superalloy CMSX-4 and silicon oxide ceramic core. Corrosion Science, 2020, 177: 108969.
[17] Zi Y, Meng J, Zou M K, et al. Effects of yttrium on wettability and interactions between molten superalloy and SiO_2-based ceramic core. Ceramics International, 2020, 46(6): 7324–7335.
[18] Chen X Y, Li Z H, Zhao Y J, et al. Wetting and interfacial phenomena between a Ni-based superalloy and silica-based ceramic cores with $ZrSiO_4$ additions. Journal of Physics: Conference Series, 2024, 2671(1): 012025.
[19] Zi Y, Meng J, Zhang C W, et al. Effect of Y content on interface reaction and wettability between a nickel-base single crystal superalloy melt and ceramic mould. Journal of Alloys and Compounds, 2019, 789: 472–484.
[20] Yao J S, Dong L P, Wang L L, et al. Interface reaction between DD6 single crystal superalloy and ceramic core. Materials Science Forum, 2021, 1035: 297–304.
[21] Yao J S, Dong L P, Wu Z Q, et al. Interfacial reaction mechanism between ceramic mould and single crystal superalloy for manufacturing turbine blade. Materials, 2022, 15(16): 5514.
[22] Liu G W, Muolo M L, Valenza F, et al. Survey on wetting of SiC by molten metals. Ceramics International, 2010, 36(4): 1177–1188.
[23] Li Q, Song J X, Wang D G, et al. Effect of Cr, Hf and temperature on interface reaction between nickel melt and silicon oxide core. Rare Metals, 2011, 30: 405–409.
[24] Lei X J, Wang X P, Kong F T, et al. The high temperature wetting and corrosion mechanism analysis of Nb by TiAl alloy melt. Corrosion Science, 2021, 186: 109316.
[25] Wang H, Shang G F, Liao J F, et al. Experimental investigations and thermodynamic calculations of the interface reactions between ceramic moulds and Ni-based single-crystal superalloys: Role of solubility of Y in the $LaAlO_3$ phase. Ceramics International, 2018, 44(7): 7667–7673.
[26] Galenko P. Gibbs free energy: Equilibrium and dynamics. Berlin: Springer International Publishing, 2024: 31–39.
[27] Chen Z A, Tan Y, Li Y, et al. Effect of oxygen on the wettability and interfacial reaction between the DD5 superalloy and ceramic shell. Vacuum, 2023, 215: 112288.